



FULL PAPER

Newly designed Mn (III)–W(V) bimetallic assembly built by manganese (III) Schiff–base and octacyanotungstate(V) building blocks: Structural topologies, and magnetic features

Mohd. Muddassir¹ | Abdullah Alarifi¹ | Mohd Afzal¹ | Nayim Sepay²

¹Catalytic Chemistry Research Chair, Department of Chemistry, College of Science, King Saud University, Riyadh, 11451, Saudi Arabia

²Department of Chemistry, Jadavpur University, Kolkata, 700032, India

Correspondence

Mohd. Muddassir, Catalytic Chemistry Research Chair, Department of Chemistry, College of Science, King Saud University, Riyadh 11451, Saudi Arabia.
Email: mmohammadarshad@ksu.edu.sa; muddassirchem@gmail.com

Funding information

Deanship of Scientific Research, King Saud University, Grant/Award Number: RG-1440-076

New complex $[\text{Mn}(\text{SB})_2(\text{DMF})_2][\text{W}(\text{CN})_8]$ hereafter referred to as complex **1**, which was prepared by self-assembly of $[\text{Mn}(\text{SB})_2(\text{DMF})_2]^{3+}$ and $[\text{W}(\text{CN})_8]^{3-}$ and structurally characterized by elemental analysis, infrared (IR) and single crystal X-ray techniques (H_2SB is Schiff base derived from the condensation of salicylaldehyde and N,N-diethylethylenediamine and DMF is dimethylformamide). The structure consists of 1-D supramolecular chains and further stacks to give a 3-D supramolecular architecture whose molecular fragments are linked by hydrogen bond as well as C–H \cdots π interactions between $[\text{Mn}(\text{SB})_2(\text{DMF})_2]^{3+}$ and $[\text{W}(\text{CN})_8]^{3-}$. An underlying net for the representation consists of two types of fragments with 1,4 M5–1 and 1,8 M9–1 topologies and further illustration of the molecular network in terms of a graph–theory approach using simplification procedure resulted in the underlying net of 2C1topological type in the complex **1**. Magnetic susceptibility measurements of complex **1** was carried out in the temperature range 2–300 K, indicates the presence of either magnetic anisotropy zero field splitting, the effect of intramolecular interactions, or both. Complex **1** follows the Curie–Weiss law with Curie constant value of $3.43 \text{ cm}^3 \text{ mol}^{-1} \text{ K}$, and the slight negative Weiss constant (-0.60 K) value indicates the predominant antiferromagnetic magnetic exchange interactions.

The magnetic properties of Title complex was investigated thoroughly and showed that ferromagnetic interaction between W(V) and Mn (III) operate *via* the intramolecular H–bonding interaction between cyanide nitrogens and a hydrogen atom.

KEYWORDS

H-bonding; magnetism, Octacyanotungstate(V), Schiff base, X-ray crystallography

1 | INTRODUCTION

In the past few decades, considerable efforts have been given to create new molecule–based magnets *via* a combination of dissimilar paramagnetic metal ions within the

same molecular unit, as the magnetic interaction between these spin carriers can be easily controlled to obtain materials with desired properties.^[1–13] A lot of large and ultra–large complexes with controlled nuclearity based on *d*– and *f*–metal centers have been

synthesized as SMMs. One such example is a family of heterometallic architecture containing polycyanometallates of Mo(V), Nb(V), or W(V),^[14] which have been employed to synthesize cyano-bridged magnetic complexes with fascinating magnetic properties, such as the T_C 's magnets,^[15–18] single-molecule magnets (SMMs),^[19–25] and single chain magnets SCMs).^[26–28] Besides, these building components materialize well appropriate to obtain low dimensional architectures such as chains.^[29–32] Our interest in this field concerns the heterometallic architectures that behaves as magnet at low temperatures; in other words, their field-induced magnetization relaxes slowly, even upon removal of the applied direct current (*dc*) field.

Many molecules are displaying SMM property, but the majority of them being Mn (III) complexes. This is because Mn (III) complexes often show relatively large ground state *S* values, as well as relatively large (and negative) *D* values associated with the presence of Jahn–Teller, distorted Mn (III) atoms. The complexes self-assembled by Mn (III)–(Schiff bases) are always of great interest because of the above-said reason. Thus far, many relevant magnetic complexes, including some SMMs and SCMs, have been reported.^[19,20,33–41] Some results have been reported in which Mn (III)–Schiff bases act as the precursors in cyanide-bridged complexes. The position and size of the substituted groups on the Schiff base ligands have been revealed to play an essential role in determining the structure of resulting complexes.^[42,43] These findings have triggered the investigation of new molecular complexes based on manganese metal ions. However, compared with solely *3d* (mainly Mn (III))–based magnetic systems, magnetic assemblies with enhanced exchange couplings and anisotropic properties can be constructed with heterometallic *4d/5d* metal ions, because they possess more radially extended orbitals and exhibit greater spin–orbit coupling. They can build a wide variety of molecular architectures from 0D to 3D depending on the coordination versatility to *3d* transition metal ions in self-assembly.^[36,44–46] Cyano-bridged metal assemblies based on octacyanometallates $[M(IV)/(V)(CN)_8]^{4-/3-}$ ($M = Mo, W$ and Nb)^[47,48] have drawn particular attention in the design and synthesis of the new molecule-based magnets because the cyanide bridge can mediate strong coupling interactions between the metal ions.

From a synthetic and magnetic point of view, Schiff-base ligands is a good choice to develop enticing metal complexes because it contains multidentate donor atoms and can coordinate to many metal centers and also the phenolic group can display a variety of bonding geometries such as monodentate, bidentate,

bridging and chelate bridging resulting in exciting magnetic property.^[49] Ashutosh Ghosh et al.,^[50] has reported two Mn (III) complexes by using Schiff base with sodium azide exhibiting interesting magnetic properties. Inspired from his results and being motivated from our previous studies of octacyanometallate-based magnets, we construct magnetic materials by replacing the sodium azide with $W(CN)_8$ ions since this may improve the magnetic properties because $W(CN)_8$ can mediate magnetic exchange interaction as it can adopt three different spatial configurations (e.g., square antiprism (D_{4h}), dodecahedron (D_{2d}), and bicapped trigonal prism (C_{2v}) depending on their chemical environment [32]. More importantly, these complexes lead to a significant increase of the exchange interactions with respect to *3d* ions cyanometallates, and also an enhanced exchange interaction may be expected due to the increased overlap between the diffuse orbitals of octacyanotungstate with Mn (III) metal ion.^[51–53] All of these merits make octacyanotungstate a promising candidate in comparison to diamagnetic sodium azide. As part of our effort in this direction, herein, we describe the syntheses, characterization, and magnetic properties of self-assembly of octacyanotungstate with Mn (III)–(SB), which proceeds to give 1-D arrangement of the building blocks employed.

2 | EXPERIMENTAL SECTION

2.1 | Physical measurements

The IR spectra were recorded with a VECTOR 22 spectrometer using KBr pellets in the 200–4,000 cm^{-1} region. Elemental analyses of C, H and N were performed on a PerkinElmer 240C elemental analyzer. TGA/DSC was performed on Universal V3.8 B TA SDT Q600 Build 51 thermal analyzer under a nitrogen atmosphere using alumina powder as the reference material. The data of magnetic properties for crystalline samples were collected on a Quantum Design MPMP-XL 7 superconducting quantum interference device (SQUID) magnetometer. Corrections of magnetic susceptibilities were carried out considering both the sample holder as the background and the diamagnetism of the constituent atoms estimated from Pascal's constant.

2.2 | Starting materials

Chemicals and solvents were purchased from commercial sources as analytical reagents and used without further

purification. $[\text{HN}(n\text{-C}_4\text{H}_9)_3]_3\text{W}(\text{CN})_8 \cdot 2\text{H}_2\text{O}$ was prepared according to the literatures procedure.^[54]

Caution! Cyanides are hyper-toxic and hazardous, thus, should be handled in small quantities and with great caution!

2.2.1 | Synthesis

The unprotonated Schiff base ligand (H_2SB) was prepared by refluxing salicylaldehyde (0.1 ml, 1 mmol) with *N,N*-Diethylethylenediamine (0.116 ml, 1 mmol) in methanol (10 ml) for 30 min. The resulting dark yellow solutions of Schiff base ligand was subsequently used for complex formation.

2.2.2 | Synthesis of complex 1

At room temperature, 0.1 mmol of methanolic solution of Schiff base ligand (2 ml) was added to a 3 ml methanolic solution of $\text{Mn}(\text{OAc})_2 \cdot 4\text{H}_2\text{O}$ (0.0245 g, 0.1 mmol) followed by a methanolic solution (2 ml) of $[\text{HN}(n\text{-C}_4\text{H}_9)_3]_3\text{W}(\text{CN})_8 \cdot 2\text{H}_2\text{O}$ (0.0329 g, 0.033 mmol). The solution turned brown, and precipitation occurs. The brown precipitate was dissolved using ca. 2 ml of DMF. The mixture was kept unstirred in a refrigerator. The red-colored, X-ray quality, prismatic shaped single crystals started to separate within a few hours and were collected after two days. Yield 28%. Elemental analysis for $\text{C}_{40}\text{H}_{54}\text{MnN}_{14}\text{O}_4\text{W}$: C 46.48, H 5.27, N 18.97%; found: C 46.23, H 5.18, N 18.93%.

2.3 | X-ray structure determination

X-Ray crystal structure determination has been given in supporting information in detail. Details of the crystallographic data collection, structural determination, and refinement are summarized in Table 1. Selected bond distances and angles are listed in Table S1. Data can also be obtained free of charge in *cif* format by request from The Cambridge Crystallographic Data Centre at www.ccdc.cam.ac.uk/data_request/cif.

3 | RESULTS AND DISCUSSION

3.1 | Synthetic strategy

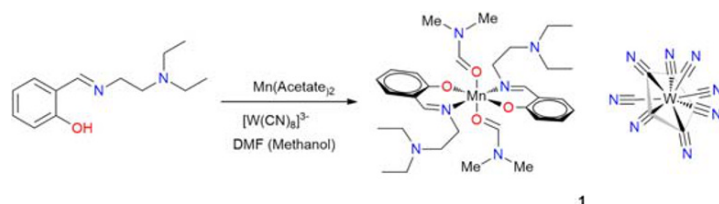
The new Mn^{III} complex (complex 1) has been prepared with the tridentate Schiff base (SB) ligands (which in our case act as bidentate) with manganese (II)

TABLE 1 Crystal structural data and refinement parameters for complex 1

CCDC No	1,977,017
Formula	$\text{C}_{40}\text{H}_{54}\text{MnN}_{14}\text{O}_4\text{W}$
Formula weight	1033.76
Temperature/K	293(2)
Crystal system	triclinic
Space group	$P - 1$
$a/\text{\AA}$	10.4518 (12) \AA
$b/\text{\AA}$	12.8571 (15) \AA
$c/\text{\AA}$	17.325 (2) \AA
$\alpha/^\circ$	78.931 (2)°
$\beta/^\circ$	89.489 (2)°
$\gamma/^\circ$	81.742 (2)°
Volume/ \AA^3	2260.7 (5)
Z	2
$\rho_{\text{calc}}/\text{mg mm}^{-3}$	1.519
μ/mm^{-1}	2.877
$F(000)$	1,046
Crystal size/ mm^3	0.25 × 0.22 × 0.2
Reflections collected	14,886
Independent reflections	10,142 [$R(\text{int}) = 0.0308$]
Data/restraints/parameters	10,142/0/552
Goodness-of-fit on F^2	0.985
Final R indexes [$I > 2\sigma(I)$]	$R_1 = 0.0425$, $wR_2 = 0.0940$
Final R indexes [all data]	$R_1 = 0.0586$, $wR_2 = 0.1015$
Largest diff. Peak/hole/ $e \text{\AA}^{-3}$	1.93/−2.18

^a $R_1 = (\sum||F_o| - |F_c||)/\sum|F_o|$. ^b $wR_2 = [\sum[w(F_o^2 - F_c^2)^2]/\sum[w(F_o^2)^2]]^{1/2}$, where $w = 1/[\sigma^2(F_o^2) + (aP)^2 + bP]$.

acetate followed by the reaction with $[\text{HN}(n\text{-C}_4\text{H}_9)_3]_3\text{W}(\text{CN})_8 \cdot 2\text{H}_2\text{O}$ in methanol/DMF under ambient conditions as red crystalline solids within a few hours, containing all coordinately isolated molecules on keeping the solutions in a refrigerator as shown in Scheme 1. Regardless of reaction ratios of Mn (SB) and $[\text{HN}(n\text{-C}_4\text{H}_9)_3]_3\text{W}(\text{CN})_8 \cdot 2\text{H}_2\text{O}$ the same coordinately isolated molecule was always obtained. On reaction with Schiff base ligand, Mn (II) was readily oxidized in the air to Mn (III) and stabilized by complex formation. The complex is stable towards air and moisture. As per our expectation, the applied synthetic strategy to the formation of complex 1 by introducing the steric hindrance at Schiff base ligand may prevented the formation of cyano-bridged complex. Since the $[\text{Mn}(\text{SB})_2(\text{DMF})_2]^{3+}$ and $[\text{W}(\text{CN})_8]^{3-}$ are isolated, attempts to connect through cyanide-bridged by changing solvents, different organic bases such as



SCHEME 1 Synthetic route for complex 1

NEt₃, NMe₄OH, NaOH and also by increasing the time duration/temperature of the reaction mixture, but all of our efforts were unsuccessful and led to the same product, as established by means of initial cell check of X-ray diffraction and IR. In a similar report, Hong, *et al.* synthesized a unique isolated W(V)–Mn(III) bimetallic compounds using different Schiff–base in acetonitrile but a similar method, which indicates the feasibility of the synthetic procedure.^[55] We also measured the TGA and its data revealed that one of the DMF solvent molecules (calcd 6.7%) is lost before complex 1 begins to decompose at around 180 °C (Figure S1) consistent with other previously reported W(V)-based complexes.^[56]

3.2 | Structure description

The asymmetric unit of complex 1 is shown in Figure 1a and the unit cell packing of the self-assembled molecular framework inside the crystal is given in Figure 1b. The crystallographic data collection and structural refinement are listed in Table 1, while, bond distances and bond angles are given in Table S1. The single X-ray diffraction analyses revealed that complex 1 includes two different metal atoms {Mn(III) and W(V)} (Figure 1a). In the [Mn(SB)₂(DMF)₂]³⁺ part, the two aromatic rings and the metal ion are almost coplanar and the oxygen atoms of both the SB stay outside of the plane with C₂ symmetry. The space group is *P* – 1 and the unit cell packing of the self-assembled [W(CN)₈]³⁻ and [Mn(SB)₂(DMF)₂]³⁺ inside the crystal is shown in Figure 1b.

Both Mn(III) metal atoms occupy a distorted octahedral coordination sphere (Figure S2a) coordinated to the one molecule of SB ligand, one molecule of DMF, and the other half set of Schiff base ligand and DMF molecule were generated through a center of symmetry. In case of Mn1 coordination sphere being equatorially coordinated to the Schiff base ligand through N9, O1, and axially coordinated to DMF O2, similarly in case of Mn2, the coordination through Schiff base ligand is N12, O3 and DMF are O4. Around Mn1 and Mn2, all similar atoms are attached in a *trans*- configuration. The W(V) center have a square antiprism molecular geometry (Figure S2b). The bond length and angles are nearly the same in both Mn(III) centers. The Mn – O_{DMF} = 2.242(4) Å and Mn – O_{ph} = 1.867(3) Å bond distances are similar in both the Mn(III) metal centers, all being common coordination bonds as reported by a similar type of Mn(III) complexes,^[50] whereas the only difference is the distance of imine nitrogen. In the case of Mn1 the Mn – N_{imine} bond distance is 2.052(4) Å, while in the latter case, it was found to be 2.061(4) Å heterometallic are in the normal range (Table S1). The oxidation states of Mn(III) metal ions were deduced from the metric parameters and charge balance consideration, which was further confirmed by bond valence sum (BVS) calculations (Table 2).

TABLE 2 BVS calculations for complex 1

[Mn(SB) ₂ (DMF) ₂] [W(CN) ₈]	Mn ²⁺	Mn ³⁺	Mn ⁴⁺
Mn1	3.2245662	3.0111414	3.0610468
Mn2	3.1967996	2.9842608	3.0352342

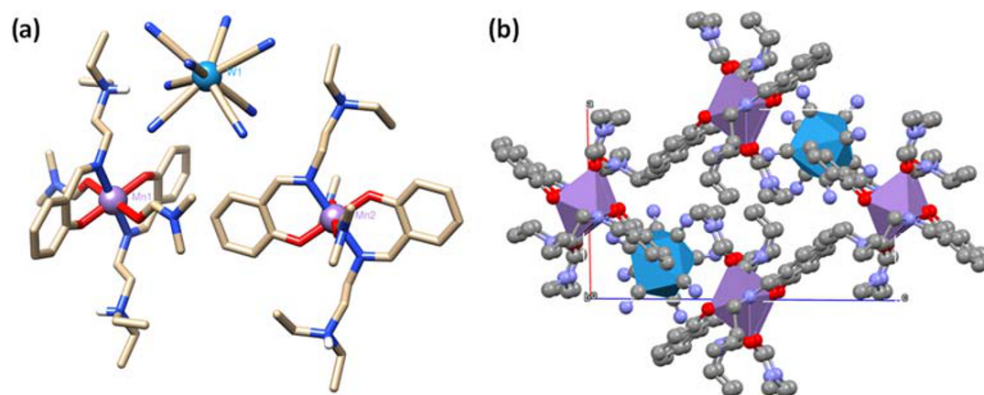


FIGURE 1 (a) Crystal structure of complex 1. (b) Packing of the self-assembled [W(CN)₈]³⁻ and [Mn(SB)₂(DMF)₂]³⁺ inside the crystal (H – atoms omitted for clarity)

The assignment of both Mn (III) centers based on bond distances is in line with the BVS values. The overall coordination geometry around Mn (III) may, therefore, be described as an elongated octahedron, which is expected from the Jahn–Teller distortion. The four donor atoms in the equatorial plane O1, N9, O1ⁱ and N9ⁱ (in case of Mn1) and O3, N12, O3ⁱ and N12ⁱ (in case of Mn2) are in the same plane and both Mn (III) atoms are almost planar from this plane. The phenyl rings are coplanar to each other in each Mn (III) center. Moreover, the equatorial O1—Mn1—N9 bond angle involving the O_{ph} and N_{imine} groups [90.51 (15)°], while in case of O3—Mn2—N12 [89.98 (15)°] is nearly equal to the angle of an ideal octahedron (90°), whereas the other equatorial N9—Mn1—O2 bond angle involving O_{DMF} and N_{imine} groups [88.96 (14)°], and N12—Mn2—O4 [92.72 (15)°] is slightly deviated from perfect octahedron (Table S1).

Self-assembly of [W (CN)₈]³⁻ and [Mn (SB)₂(DMF)₂]³⁺ form 1-D chain whose molecular fragments are linked by hydrogen bonds between cyanide nitrogen and a hydrogen atom, which is connected with positively charged quaternary nitrogen (Figure 2a). Interestingly, the two adjacent [Mn (SB)₂(DMF)₂]³⁺ units are neither parallel nor perpendicular to each other at an angle 67.20° between two such [MnDMF (SB)] units (Figure S3). The one-dimensional chain of Mn (III) units can elongate infinitely along the unit cell axis b. The 67.20° tilting situation of the Mn (III) part allows more moiety to interact with CN⁻ groups. The alkyl chains attached to the SB and CN⁻ group of [W (CN)₈]³⁻ plays a prominent key role in the assembling process. Besides, the 3D supramolecular architecture of complex **1** was generated, which exhibits strong C – H...π interactions between alkyl and imine hydrogens of SB moieties and

available CN⁻ groups and stabilizes the crystal structures (Figure 2b). It is worth nothing to mention that the improper dihedral angles of the two methyl groups of –NHET₂ are 100.89° instead of zero (Figure S4). This conformational preference at 100.89° allows both carbons of each the ethyl groups to form C – H...π interactions with different CN⁻ nitrogen atoms. In this way, one [W (CN)₈]³⁻ unit can interact with alkyl chains of five different Mn (SB) units (Figure 2b) and able to stabilize the three-dimensional framework of their 1 – D molecular assembly. The geometry of W(V) metal ion deserves particular attention because W (CN)₈ polyhedron has a significant incidence on the strengths of the exchange interaction.^[57]

The geometry of W(V) center surrounded by eight C atoms from the CN⁻ groups has been analyzed with the SHAPE program,^[58] revealing a distorted square antiprism (SAPR–8), the results being tabulated in Table S2. N1N2N3N4 and N5N6N7N8 comprise the two square basic planes of the antiprism with the mean deviations of 0.144, and 0.256 Å from each plane, respectively, and their dihedral angle is 1.6°. The distances of W(V) to the N1N2N3N4 plane center and N5N6N7N8 plane center are 1.754(4) and 1.785(3) Å, resulting in the difference Δd = 0.031 Å, whereas the related Δd for [W (CN)₈]³⁻ is 0.418 Å (Figure 3).

The W – C bond lengths range from 2.149(6) to 2.183(5) Å, and the C ≡ N bond lengths from 1.124(7) to 1.144(7) Å. The W – C ≡ N linkages are almost linear, with the angles ranging from 177.0 (6) to 179.4 (6)°. All bond lengths and angles in [W (CN)₈]³⁻ in the complex **1** are comparable with those in reported kinds of literature.^[47,59,60] The Mn – Mn separation within the complex is 10.077(11) Å, while the distance between each Mn1 – W1

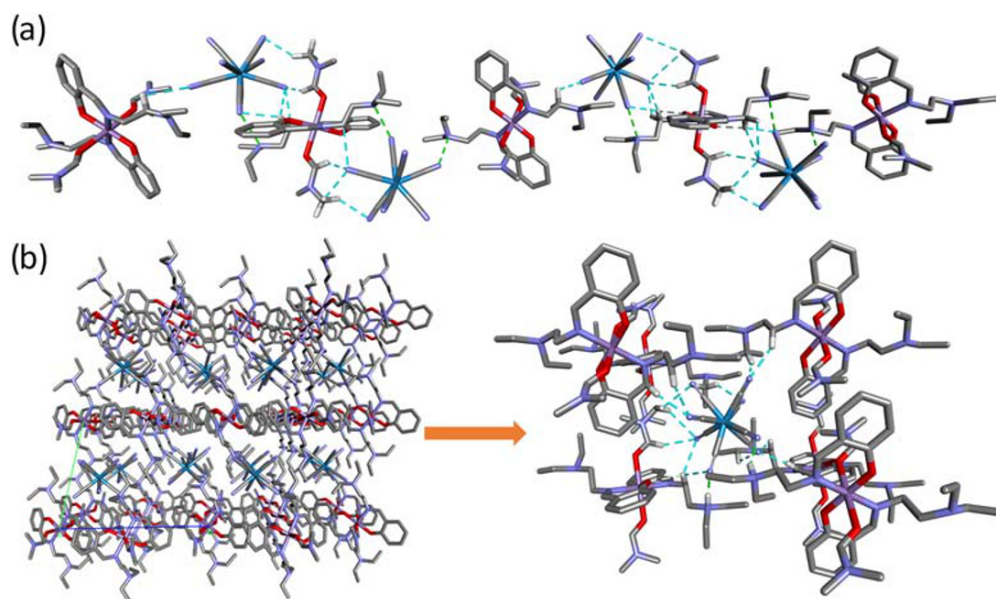


FIGURE 2 (a) 1D chain of complex **1** along b – direction. (b) 3D packing of [Mn (SB)₂(DMF)₂]³⁺ and [W (CN)₈]³⁻ inside the unit cell and hydrogen bonding as well as C – H ... π interactions (H-atoms omitted for clarity)

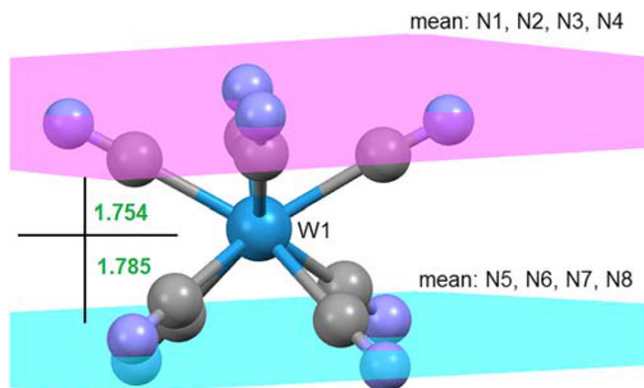


FIGURE 3 The square antiprism geometry of W(V) center

and Mn2 – W2 is 7.482(13) Å and 8.406(8) Å, respectively, whereas the bond angle is 78.49(3)°. It is worth noting that the intermolecular distance could be a major influencing factor of the magnetic properties in these complexes.

The topological analysis for complex **1** was performed with the ToposPro program which is the keystone of the topological analysis for structure representation and the TTD collection of periodic network topologies.^[61,62] The universal approach to the crystal structure description is to consider all atoms, and all (even weakest) links between them, which corresponds to the complete representation, any other representation with a derived topology is partial. The topology of a partial representation is described by an underlying net in the so-called standard representation of the valence-bonded MOFs.^[63,64] The structural building units for complex **1** showing an underlying net for the description consists of two types of fragments with 1,4 M5-1 and 1,8 M9-1 topological type whose nodes correspond to all metal atoms and the centers of mass of the organic ligands in the representation of the underlying net (Figure S5). The standard topological representation of complex **1** can be described as a chain of an underlying net of 2C1 topological type whose nodes correspond to $[\text{Mn}(\text{SB})_2(\text{DMF})_2]^{3+}$ and $[\text{W}(\text{CN})_8]^{3-}$, respectively in a self-assembled molecular framework (Figure 4).

In order to further execute the multilevel topological explanation [65] of the molecular packing, we select the value of molecular solid angle (Ω_i) as a criterion, which will serve as a weight factor to be proportional to the strength of the intermolecular contact. Using the subroutine generate representations implemented in ToposPro, different subnets (important building blocks of the internet topology) can be obtained from the underlying net of 2C1 topological type that contains the edges of weight no less than a specified value (Figure 5).

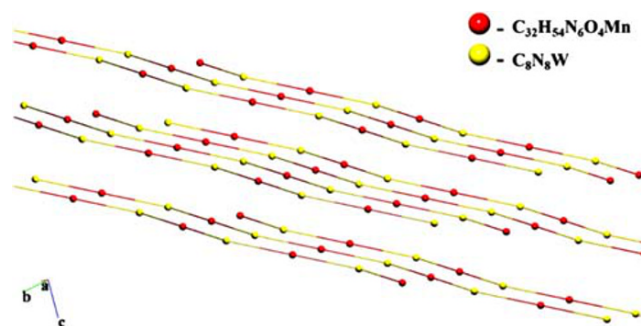


FIGURE 4 The standard representation of the H – bonded molecular MOFs in the complex **1**. The underlying net of 2C1 topological type obtained after secondary simplification. Red and yellow spheres correspond to $[\text{Mn}(\text{SB})_2(\text{DMF})_2]^{3+}$ and $[\text{W}(\text{CN})_8]^{3-}$, respectively

Each subnet of this net contains information about the spatial arrangement of strong intermolecular contacts, assuming the Ω_i is proportional to the strength of intermolecular interaction (Table S3).

3.3 | FT-IR Spectrum

In the spectra of the free salicylaldehyde ligands, the intense bands stemming from the stretching and bending vibrational modes of the phenolic –OH around 3,200 cm^{-1} and 1,410 cm^{-1} , respectively, disappear from the spectra of the complex **1** indicating the ligand deprotonation.^[66] Also, the bands originating from the C – O stretching vibrations were observed at 1243–1295 cm^{-1} in the complex **1**. The band at 3400 cm^{-1} has been assigned to the –NH stretching vibration of the complex,^[67] and its broad feature is attributed to the formation of hydrogen bonding as reported in literature by similar complexes^[55] while the bending mode of N – H is present at 1547 cm^{-1} . Ghosh *et al.*^[50] has also reported similar band but shorter wavelength than title complex probably because absence of hydrogen bonding. The band at ~1,611 cm^{-1} attributable to the $\nu(-\text{CH}=\text{N})$ of the Schiff base ligand, coordinated to Mn center. The stretching frequencies of the –C=O bonds are located at 1643 cm^{-1} which are related to the coordinated DMF molecule.^[68] The medium to low intensity bands at 640 and 444 cm^{-1} are attributed to the coordination bonds (Mn – O and Mn – N, respectively) according to the literature^[69] The $[\text{W}(\text{CN})_8]^{3-}$ based characteristic CN bands in the IR data occur at 2155sh and 2,138 cm^{-1} for complex **1**. The broad absorptions are centered around 3,400 indicates that hydrogen bonds are involved in the complex.

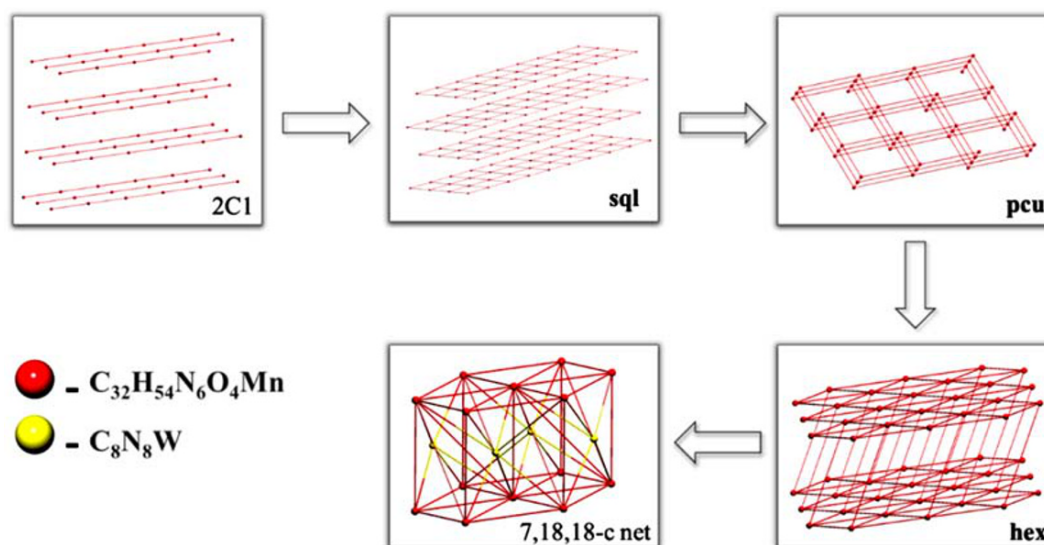


FIGURE 5 Subnets of the initial net corresponding to the molecular packing in structure at different levels: 2 – c 2C1 \rightarrow 4 – c sql \rightarrow 6 – c pcu \rightarrow 8 – c hex \rightarrow 7,18,18 – c net

3.4 | Magnetic properties

Variable-temperature dc magnetic susceptibility data for complex **1** was collected in the temperature range 2–300 K under an applied field of 2000 Oe. The $\chi_M T$ versus T data, where χ_M is the molar magnetic susceptibility and T is the absolute temperature, is shown in Figure 6a. The observed $\chi_M T$ value at 300 K of $3.412 \text{ cm}^3 \cdot \text{K} \cdot \text{mol}^{-1}$ for **1** is slightly higher to the expected value of $3.375 \text{ cm}^3 \cdot \text{K} \cdot \text{mol}^{-1}$ for a non-interacted spin system of two-half Mn (III) ion ($S = 2$, $C = 3 \text{ cm}^3 \cdot \text{K} \cdot \text{mol}^{-1}$ with $g = 2$) and one W(V) ion ($S = \frac{1}{2}$, $C = 0.375 \text{ cm}^3 \cdot \text{K} \cdot \text{mol}^{-1}$ with $g = 2$). The magnetic data show that $\chi_M T$ remains almost constant up to 90 K. Below the cusp temperature, the $\chi_M T$ product drastically drops and reach a minimum of

$2.50 \text{ cm}^3 \cdot \text{K} \cdot \text{mol}^{-1}$. This nature of the $\chi_M T$ plot suggests a weak antiferromagnetic coupling between paramagnetic Mn (III) and W(V) centers through H-bonding. The faster decrease in a low-temperature region denotes the presence of magnetic anisotropy zero-field splitting (quite remarkable in Mn (III) centers), the effect of intramolecular interactions, or both,^[70] but, the contribution of weak antiferromagnetic interactions cannot be ruled out.

The magnetic data of complex **1** obey the Curie–Weiss law [$\chi_M = C/(T - \theta)$] very well, where C and θ are Curie and Weiss constants, respectively affording $C = 3.43 \text{ cm}^3 \text{mol}^{-1} \text{K}$ and $\theta = -0.60 \text{ K}$ (Figure 6b).

The Curie constant is in good agreement with the expected value of $3.375 \text{ cm}^3 \text{mol}^{-1} \text{K}$. The overall shape of the $\chi_M T$ versus T curve of the 1.8–300 K region and

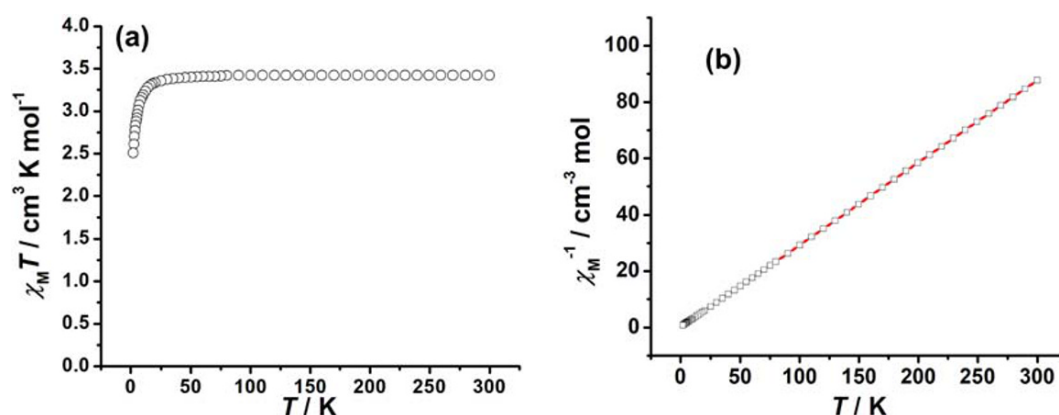


FIGURE 6 (a) Temperature dependence of the $\chi_M T$ product under an applied field of 2000 Oe. (b) Plot of χ_M^{-1} vs T for complex **1** at 2000 Oe applied field with the linear fit shown as a red line

the negative Weiss constant value indicates the predominant antiferromagnetic magnetic exchange interactions. This manifests that the isolated metal centers are antiferromagnetically correlated through the hydrogen bonds.

To gain more insight into the magnetic behavior at low temperatures, field cooled (FC) magnetic susceptibility measurements (Figure S6) were performed from 2–300 K under 2000 Oe applied field. Below 20 K, the FC magnetization curve shows a gradual increase and changes its slope further at 9.0 K and shows no saturation effect until the lowest measured temperature. This shows the presence of an uncompensated spin below this temperature, which contributes to this net magnetization.

The dynamic magnetic properties of complex **1** were further probed by alternating-current (ac) measurements in the temperature range 1.9–7 K, as shown in Figure S7. Under a zero dc field and a 5 Oe ac field oscillating at frequencies between 1 and 1,500 Hz, no ac signal was observed. However, when a static dc field (2,500 Oe) was applied, complex **1** displayed a frequency-independent in-phase (χ') and frequency-dependent out-of-phase (χ'') signal, and signal presents two peaks or a peak and a shoulder (in case of χ'') at frequencies above than 1,000 Hz at 1.9 K, indicates weak magnetic coupling or possibly the slow relaxation of magnetization.

$[\text{W}(\text{CN})_8]^{3-}$ can usually mediate the stronger magnetic interaction between metal ions than N_3^- due to the more extensive diffusion of the 5d orbitals (heavy-atom effect). However, comparing with the similar complexes in the literature, the title complex exhibits very weak magnetic coupling, which can be attributed to the difference in the structure.

4 | CONCLUSIONS

New complex **1** with the one-dimensional supramolecular framework have been prepared by self-assembling $[\text{W}(\text{CN})_8]^{3-}$ and the respective Mn (III) Schiff base complex that are linked *via* hydrogen bonds between cyanide groups and imine groups of both Mn (III) units and thoroughly characterized, all of our attempts to connect through cyanide-bridged by different methods were unsuccessful and led to the same isolated product. The magnetic properties of Complex **1** were investigated thoroughly. They showed that antiferromagnetic interaction between W(V) and Mn (III) operates *via* the intramolecular H-bonding interaction between cyanide nitrogens and a hydrogen atom, slight negative Weiss constant (−0.60 K) value further indicates the predominant antiferromagnetic magnetic exchange interactions.

Efforts to construct other fascinating structures by reacting to the current Schiff base ligand (SB) and other less hindered Schiff bases with other transition metal salts, as well as other rare-earth (III), salts together with octacyanomometallates are continuing in our laboratory.

ACKNOWLEDGEMENTS

The authors would like to extend their sincere appreciation to the Deanship of Scientific Research at King Saud University for funding this work through research group project number RG-1440-076.

CONFLICT OF INTEREST

The author declares no conflict of interest.

ORCID

Mohd. Muddassir  <https://orcid.org/0000-0001-7069-2557>

Nayim Sepay  <https://orcid.org/0000-0001-7702-3989>

REFERENCES

- [1] K. Bhattacharjee, S. P. Pati, G. C. Das, K. K. Chattopadhyay, *Cryst. Growth Des.* **2017**, *17*, 719.
- [2] G. Bhargavi, M. V. Rajasekharan, J.-P. Costes, J.-P. Tuchagues, *Dalt. Trans* **2013**, *42*, 8113.
- [3] S. Vaidya, S. Tewary, S. K. Singh, S. K. Langley, K. S. Murray, Y. Lan, W. Wernsdorfer, G. Rajaraman, M. Shanmugam, *Inorg. Chem.* **2016**, *55*, 9564.
- [4] P. Pandey, S. Tripathi, M. Shanmugam, R. J. Butcher, S. S. Sunkari, *Inorganica Chim. Acta* **2019**, *495*, 118997.
- [5] J. Qian, J. Hu, H. Yoshikawa, J. Zhang, K. Awaga, C. Zhang, *Cryst. Growth Des.* **2014**, *14*, 2288.
- [6] Y.-L. Bai, X. Bao, S. Zhu, J. Fang, J. Tao, *Dalt. Trans.* **2013**, *42*, 1033.
- [7] Y.-M. Li, X.-F. Li, Y.-Y. Wu, D. L. Collins-Wildman, S.-M. Hu, Y. Liu, H.-Y. Li, X.-W. Zhao, L.-Y. Jin, D.-B. Dang, *Cryst. Growth Des.* **2018**, *18*, 7541.
- [8] R. Bagai, G. Christou, *Chem. Soc. Rev.* **2009**, *38*, 1011.
- [9] H. Zhang, C. Xue, J. Shi, H. Liu, Y. Dong, Z. Zhao, D. Zhang, J. Jiang, *Cryst. Growth Des.* **2016**, *16*, 5753.
- [10] R. Ishikawa, M. Nakano, B. K. Breedlove, M. Yamashita, *Polyhedron* **2013**, *64*, 346.
- [11] S. Vaidya, P. Shukla, S. Tripathi, E. Rivière, T. Mallah, G. Rajaraman, M. Shanmugam, *Inorg. Chem.* **2018**, *57*, 3371.
- [12] F. El-Khatib, B. Cahier, F. Shao, M. López-Jordà, R. Guillot, E. Rivière, H. Hafez, Z. Saad, J.-J. Girerd, N. Guihéry, T. Mallah, *Inorg. Chem.* **2017**, *56*, 4601.
- [13] S. Vaidya, A. Upadhyay, S. K. Singh, T. Gupta, S. Tewary, S. K. Langley, J. P. S. Walsh, K. S. Murray, G. Rajaraman, M. Shanmugam, *Chem. Commun.* **2015**, *51*, 3739.
- [14] T. S. Venkatakrishnan, C. Duhayon, N. Gogoi, J.-P. Sutter, *Inorganica Chim. Acta* **2011**, *372*, 403.

- [15] S. Tanase, F. Tuna, P. Guionneau, T. Maris, G. Rombaut, C. Mathonière, M. Andruh, J.-P. Olivier Kahn, *Sutter, Inorg. Chem.* **2003**, *42*, 1625.
- [16] J. Milon, M.-C. Daniel, A. Kaiba, P. Guionneau, S. Brandès, J.-P. Sutter, *J. Am. Chem. Soc.* **2007**, *129*, 13872.
- [17] W. Kosaka, K. Imoto, Y. Tsunobuchi, S. Ohkoshi, *Inorg. Chem.* **2009**, *48*, 4604.
- [18] K. Tomono, Y. Tsunobuchi, K. Nakabayashi, S. Ohkoshi, *Inorg. Chem.* **2010**, *49*, 1298.
- [19] H. J. Choi, J. J. Sokol, J. R. Long, *Inorg. Chem.* **2004**, *43*, 1606.
- [20] H. Miyasaka, H. Takahashi, T. Madanbashi, K. Sugiura, R. Clérac, H. Nojiri, *Inorg. Chem.* **2005**, *44*, 5969.
- [21] T. Glaser, M. Heidemeier, T. Weyhermüller, R.-D. Hoffmann, H. Rupp, P. Müller, *Angew. Chemie Int. Ed.* **2006**, *45*, 6033.
- [22] P. L. W. Tregenna-Piggott, D. Sheptyakov, L. Keller, S. I. Klokishner, S. M. Ostrovsky, A. V. Palii, O. S. Reu, J. Bendix, T. Brock-Nannestad, K. Pedersen, et al., *Inorg. Chem.* **2009**, *48*, 128.
- [23] J. Dreiser, A. Schnegg, K. Holldack, K. S. Pedersen, M. Schau-Magnussen, J. Nehrkorn, P. Tregenna-Piggott, H. Mutka, H. Weihe, J. Bendix, et al., *Chem. – A Eur. J.* **2011**, *17*, 7492.
- [24] V. Hoeke, M. Heidemeier, E. Krickemeyer, A. Stammler, H. Bögge, J. Schnack, T. Glaser, *Dalt. Trans.* **2012**, *41*, 12942.
- [25] H. Kara, A. Azizoglu, A. Karaoglu, Y. Yahsi, E. Gungor, A. Caneschi, L. Sorace, *CrystEngComm* **2012**, *14*, 7320.
- [26] M. Ferbinteanu, H. Miyasaka, W. Wernsdorfer, K. Nakata, K. Sugiura, M. Yamashita, C. Coulon, R. Clérac, *J. Am. Chem. Soc.* **2005**, *127*, 3090.
- [27] H.-B. Zhou, J. Wang, H.-S. Wang, Y.-L. Xu, X.-J. Song, Y. Song, X.-Z. You, *Inorg. Chem.* **2011**, *50*, 6868.
- [28] H. Miyasaka, T. Madanbashi, A. Saitoh, N. Motokawa, R. Ishikawa, M. Yamashita, S. Bahr, W. Wernsdorfer, R. Clérac, *Chem. – A Eur. J.* **2012**, *18*, 3942.
- [29] R. Bag, Y. Sikdar, P. Saha, P. Ghosh, M. G. B. Drew, S. Goswami, *Cryst. Growth Des.* **2020**, *20*, 1849.
- [30] H. Zhou, Q. Chen, H.-B. Zhou, X.-Z. Yang, Y. Song, A.-H. Yuan, *Cryst. Growth Des.* **2016**, *16*, 1708.
- [31] C.-B. Han, Y.-L. Wang, Y.-L. Li, C.-M. Liu, Q.-Y. Liu, *Inorg. Chem. Commun.* **2015**, *58*, 91.
- [32] S. Ikeda, T. Hozumi, K. Hashimoto, S. Ohkoshi, *Dalt. Trans.* **2005**, 2120.
- [33] X. Zheng, L. Zhou, Y. Huang, C. Wang, J. Duan, L. Wen, Z. Tian, D. Li, J. Mater, *Chem. A* **2014**, *2*, 12413.
- [34] N. Matsumoto, Y. Sunatsuki, H. Miyasaka, Y. Hashimoto, D. Luneau, J.-P. Tuchagues, *Angew. Chemie Int. Ed.* **1999**, *38*, 171.
- [35] S. W. Choi, D. W. Ryu, J. W. Lee, J. H. Yoon, H. C. Kim, H. Lee, B. K. Cho, C. S. Hong, *Inorg. Chem.* **2009**, *48*, 9066.
- [36] J. H. Yoon, J. H. Lim, H. C. Kim, C. S. Hong, *Inorg. Chem.* **2006**, *45*, 9613.
- [37] H. Miyasaka, T. Madanbashi, K. Sugimoto, Y. Nakazawa, W. Wernsdorfer, K. Sugiura, M. Yamashita, C. Coulon, R. Clérac, *Chem. – A Eur. J.* **2006**, *12*, 7028.
- [38] H.-R. Wen, C.-F. Wang, Y.-Z. Li, J.-L. Zuo, Y. Song, X.-Z. You, *Inorg. Chem.* **2006**, *45*, 7032.
- [39] W.-W. Ni, Z.-H. Ni, A.-L. Cui, X. Liang, H.-Z. Kou, *Inorg. Chem.* **2007**, *46*, 22.
- [40] F. Pan, Z.-M. Wang, S. Gao, *Inorg. Chem.* **2007**, *46*, 10221.
- [41] H. Miyasaka, A. Saitoh, S. Abe, *Coord. Chem. Rev.* **2007**, *251*, 2622.
- [42] Z.-H. Ni, L. Zheng, L.-F. Zhang, A.-L. Cui, W.-W. Ni, C.-C. Zhao, H.-Z. Kou, *Eur. J. Inorg. Chem.* **2007**, *2007*, 1240.
- [43] D. Zhang, H. Wang, Y. Chen, Z.-H. Ni, L. Tian, J. Jiang, *Inorg. Chem.* **2009**, *48*, 11215.
- [44] Y. Song, P. Zhang, X.-M. Ren, X.-F. Shen, Y.-Z. Li, X.-Z. You, *J. Am. Chem. Soc.* **2005**, *127*, 3708.
- [45] P. Przychodzeń, T. Korzeniak, R. Podgajny, B. Sieklucka, *Coord. Chem. Rev.* **2006**, *250*, 2234.
- [46] D. E. Freedman, M. V. Bennett, J. R. Long, *Dalt. Trans.* **2006**, 2829.
- [47] Z. J. Zhong, H. Seino, Y. Mizobe, M. Hidai, A. Fujishima, S. Ohkoshi, K. Hashimoto, *J. Am. Chem. Soc.* **2000**, *122*, 2952.
- [48] G. Aromí, E. K. Brechin, in (Ed.: R. Winpenny), Springer Berlin Heidelberg, Berlin, Heidelberg, **2006**, pp. 1.
- [49] H.-S. Wang, C.-L. Yin, Z.-B. Hu, Y. Chen, Z.-Q. Pan, Y. Song, Y.-Q. Zhang, Z.-C. Zhang, *Dalt. Trans.* **2019**, *48*, 10011.
- [50] S. Naiya, S. Biswas, M. G. B. Drew, C. J. Gómez-García, A. Ghosh, *Inorg. Chem.* **2012**, *51*, 5332.
- [51] C. C. Xue, H. Y. Zhang, D. P. Zhang, *Russ. J. Coord. Chem.* **2017**, *43*, 260.
- [52] J. H. Yoon, K. S. Lim, D. W. Ryu, W. R. Lee, S. W. Yoon, B. J. Suh, C. S. Hong, *Inorg. Chem.* **2014**, *53*, 10437.
- [53] C. Yang, Q.-L. Wang, C.-Y. Su, L.-N. Hu, L.-C. Li, D.-Z. Liao, *Inorg. Chem. Commun.* **2014**, *40*, 26.
- [54] L. D. C. Bok, J. G. Leipoldt, S. S. Basson, *Zeitschrift für Anorg. Und Allg. Chemie* **1975**, *415*, 81.
- [55] H. H. Ko, J. H. Lim, H. S. Yoo, J. S. Kang, H. C. Kim, E. K. Koh, C. S. Hong, *Dalt. Trans.* **2007**, 207.
- [56] Y.-Z. Zhang, B. S. Dolinar, S. Liu, A. J. Brown, X. Zhang, Z.-X. Wang, K. R. Dunbar, *Chem. Sci.* **2018**, *9*, 119.
- [57] D. Visinescu, C. Desplanches, I. Imaz, V. Bahers, R. Pradhan, F. A. Villamena, P. Guionneau, J.-P. Sutter, *J. Am. Chem. Soc.* **2006**, *128*, 10202.
- [58] D. Casanova, M. Llunell, P. Alemany, S. Alvarez, *Chem. – A Eur. J.* **2005**, *11*, 1479.
- [59] Y. Arimoto, S. Ohkoshi, Z. J. Zhong, H. Seino, Y. Mizobe, K. Hashimoto, *J. Am. Chem. Soc.* **2003**, *125*, 9240.
- [60] J. M. Herrera, V. Marvaud, M. Verdaguer, J. Marrot, M. Kalisz, C. Mathonière, *Angew. Chem., Int. Ed.* **2004**, *43*, 5468.
- [61] V. A. Blatov, A. P. Shevchenko, D. M. Proserpio, *Cryst. Growth Des.* **2014**, *14*, 3576.
- [62] M. O'Keeffe, M. A. Peskov, S. J. Ramsden, O. M. Yaghi, *Acc. Chem. Res.* **2008**, *41*, 1782.
- [63] V. N. Serezhkin, A. V. Vologzhanina, L. B. Serezhkina, E. S. Smirnova, E. V. Grachova, P. V. Ostrova, M. Y. Antipin, *Acta Crystallogr. Sect. B* **2009**, *65*, 45.
- [64] E. V. Alexandrov, V. A. Blatov, A. V. Kochetkov, D. M. Proserpio, *CrystEngComm* **2011**, *13*, 3947.
- [65] F. Aman, A. M. Asiri, W. A. Siddiqui, M. N. Arshad, A. Ashraf, N. S. Zakharov, V. A. Blatov, *CrystEngComm* **2014**, *16*, 1963.
- [66] F. Arjmand, M. Muddassir, J. Photochem, *Photobiol. B Biol.* **2010**, *101*, 37.
- [67] F. Arjmand, M. Muddassir, Y. Zaidi, D. Ray, *Med. Chem. Commun.* **2013**, *4*, 394.

- [68] M. Muddassir, X.-J. Song, Y. Chen, F. Cao, R.-M. Wei, Y. Song, *CrystEngComm* **2013**, *15*, 10541.
- [69] K. Nakamoto, *Infrared and Raman Spectra of Inorganic and Coordination Compounds*, Wiley, New York **1986**.
- [70] M. Muddassir, Y. Song, *Crystals* **2020**, *10*, 87.

SUPPORTING INFORMATION

Additional supporting information may be found online in the Supporting Information section at the end of this article.

How to cite this article: Muddassir M, Alarifi A, Afzal M, Sepay N. Newly designed Mn (III)–W(V) bimetallic assembly built by manganese (III) Schiff–base and octacyanotungstate(V) building blocks: Structural topologies, and magnetic features. *Appl Organomet Chem.* 2020;e5914. <https://doi.org/10.1002/aoc.5914>